Inorganic Chemistry

Article

pubs.acs.org/IC

Photoinduced Interactions of Supramolecular Ruthenium(II) Complexes with Plasmid DNA: Synthesis and Spectroscopic, Electrochemical, and DNA Photocleavage Studies

Shawn Swavey,* Madeleine DeBeer, and Kaiyu Li

SupraMolecular Applied Research and Technology Center, Department of Chemistry, University of Dayton, 300 College Park, Dayton, Ohio 45469-2357, United States

ABSTRACT: Two new bridging ligands have been synthesized by combining substituted benzaldehydes with phenanthrolinopyrrole (php), resulting in new polyazine bridging ligands. The ligands have been characterized by ^{1}H NMR, mass spectroscopy, and elemental analysis. These new ligands display $\pi-\pi^*$ transitions above 500 nm with modest molar absorptivities. Upon excitation at the ligand-centered charge-transfer transition, weak emission with a maximum wavelength of 612 nm is observed. When coordinated to two ruthenium(II) bis(bipyridyl) groups, the new bimetallic complexes generated give an overall 4+ charge. The electronic transitions of the bimetallic ruthenium(II) complexes display traditional $\pi-\pi^*$ transitions at 287 nm and metal-to-ligand charge-transfer transitions at 452 nm with molar absorptivities greater than 30000 M^{-1} cm^{-1}. Oxidation of the ruthenium(II) metal centers to ruthenium(III) occurs at potentials above 1.4 V versus the Ag/AgCl reference electrode. Spectroscopic and electrochemical measurements indicate that the ruthenium(II) moieties behave independently. Both complexes are water-soluble and show the ability to photonick plasmid DNA when irradiated with low-energy light above 550 nm. In addition, one of the complexes, $[Ru(bpy)_2php]_2Van^{4+}$, shows the ability to linearize plasmid DNA and gives evidence, by gel electrophoresis, of photoinduced binding to plasmid DNA.

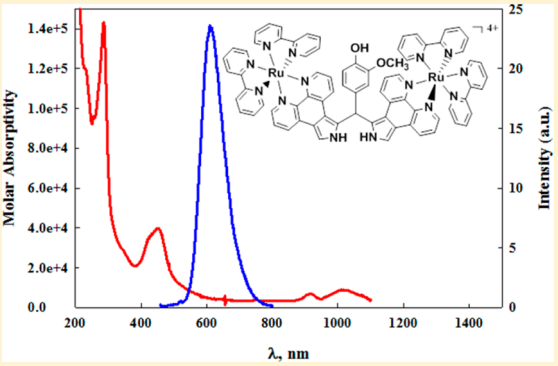

INTRODUCTION

The discovery and FDA approval of the chemotherapeutic drug cisplatin [*cis*-diaminedichloroplatinum(II)] ushered in a concerted focus on transition metals and transition-metal complexes in medicine. Since then, a number of cisplatin analogues have been approved and countless other transition-metal complexes have been evaluated for their therapeutic benefit. For the past decade, ruthenium coordination complexes and ruthenium organometallic complexes have found utility in the treatment of a variety of illnesses, including malaria,[1] bacterial infections,[1−3] and cancer.[4−13] The biological similarity of ruthenium and iron, coupled with the fact that tumor cells are rapidly growing and dividing and therefore require more iron than normal cells, has allowed researchers to develop tumor-specific ruthenium complexes.[6,7] In one case, scientists have developed a new class of ruthenium(II) arene complexes capable of taking advantage of the tumor cells' need for more iron. These new ruthenium-based drugs, referred to as RAPTA compounds, contain ligands capable of binding to transferrin.[6−8] Once in the tumor cell, it is believed that the drugs induce the cells to produce kinase inhibitors, which stop the cells' synthesis of DNA, ultimately leading to cell death. Other anticancer ruthenium(II) arene complexes inhibit carbonic anhydrase, preventing tumor cells from converting carbon dioxide into bicarbonate and hydrogen ions.[14] In another study, ruthenium(II) coordinated to crown thioethers capable of dissociating under the physiological conditions of the tumor cells, resulting in the inhibition of topoisomerase and preventing tumor cell division.[15]

Ruthenium(III) complexes have also been studied as anticancer agents; for example, *cis*-$[RuCl_2(NH_3)_4]Cl$ stimulates tumor cell apoptosis at higher doses, but in lower doses, it induces the proliferation of cancer-fighting T-cells.[16] Another widely studied ruthenium(III) complex referred to as KP1019 [*trans*-tetrachloridobis(1*H*-indazole)ruthenate(III)] has been shown to undergo selective uptake in tumor cells, binding to DNA and inhibiting transcription, which results in tumor cell death.[11,12] A similar complex that is, like KP1019, currently in clinical trials is NAMI-A, an octahedral ruthenium(III) complex coordinated to an imidazole ligand, four chlorides in the equatorial plane, and dimethyl sulfoxide (DMSO) trans to the imidazole.[17] Both KP1019 and NAMI-A are selective toward tumor cells and undergo reduction to ruthenium(II) within the reducing environment of the tumor cells, thus activating the complexes toward cell apoptosis.[18] In clinical trials, these complexes have been found to be effective against metastatic tumor cells.[17,18] These studies indicating the tumor selectivity of ruthenium complexes has made them attractive candidates as photosensitizers for use in photodynamic therapy (PDT).

Received: September 30, 2014
Published: March 23, 2015

DOI: 10.1021/ic502340p
Inorg. Chem. 2015, 54, 3139−3147

Ruthenium(II) polyazine complexes, with their rich photophysical and stable redox properties under physiological conditions, have received a great deal of attention as biological probes and light-activated therapeutics.[19−21] As a result, it has been noted that a key component of the photoreactivity of these complexes with nucleic acids lies in the reactivity of the triplet metal-to-ligand charge-transfer (^{3}MLCT) state.[22] Although the triplet metal-centered (^{3}MC) state is thermally accessible by the ^{3}MLCT, photoreactions from the ^{3}MC state of these complexes are rare.[23,24] The photoreactivity resulting from the ^{3}MLCT is not, however, the result of electron transfer from the excited ruthenium complex to the nucleic acids but the ability of the vacated electron hole to accept electrons from the nucleic acids, thereby acting as an oxidizing agent.[19,25−28] This has led researchers to look at polyazine ligands capable of stabilizing the t_{2g} orbitals of the ruthenium center, for example, 1,10-phenanthroline and 2,2′-bipyridine. Of particular interest to this laboratory are DNA photoreactions of supramolecular multimetallic ruthenium(II) polypyridyl complexes. Polyazine bridging ligands such as 2,2′-bipyrimidine, 2,3-bis(2-pyridyl)-pyrazine, 1,4,5,8,9,12-hexaazatriphenylene (HAT), and 1,10-phenanthroline[5,6-*b*]1,4,5,8,9,12-hexaazatriphenylene (PRE-HAT) have represented the lion's share of multimetallic ruthenium bridging units over the past 2 decades.[29−36] These ridged highly aromatic bridging ligands offer stabilization of the Ru(dπ) orbitals along with the intrinsically higher MLCT molar absorptivities. Other bridging ligands have been designed to take advantage of long-range DNA interactions by separating the bridging ligand with saturated alkyl chains and, as a result, increasing the hydrophobicity of the molecules, thereby enhancing their ability to cross cellular membranes.[37,38]

This report describes the synthesis and spectroscopic and electrochemical characterization of two new substituted methylene-bridged phenanthrolinopyrrole ligands. These bridging ligands combine the delocalized π systems associated with polyazine bridging ligands with saturated methylene bridging groups, resulting in interesting ligand-based photophysical properties. The coordination of ruthenium(II) polypyridyl moieties results in two new bimetallic ruthenium(II) complexes; their spectroscopic and electrochemical properties are presented. In addition, aqueous solutions of the diruthenium(II) complexes show the ability to photoreact with plasmid DNA when irradiated with low-energy light.

EXPERIMENTAL SECTION

Materials. All reagents were used as received without further purification. The precursors $RuCl_3$ trihydrate and 5-nitro-1,10-phenanthroline were purchased from Aldrich, as was tetrabutylammonium hexafluorophosphate (Bu_4NPF_6, used as the supporting electrolyte for electrochemical measurements). Ethyl isocyanoacetate, ammonium hexafluorophosphate, 1,8-diazabicyclo[5,4,0]undec-7-ene, 4-cyanobenzaldehyde (4-CNPh), 4-hydroxy-3-methoxybenzaldehyde, anhydrous tetrahydrofuran, 2,2′-dipyridyl, ethylene glycol, dimethyl-d_6 sulfoxide, ammonium hydroxide, acetic acid, ammonium hexafluorophosphate, and acetonitrile were purchased from Acros. Anhydrous ethanol, potassium hydroxide, *N*,*N*′-dimethylformamide (DMF), tris(hydroxymethyl)aminoethane (Tris) base, boric acid, chloroform, methanol, diethyl ether, silica gel (32−63 μm), ethidium bromide (EthBr), and agarose low EEO were purchased from Fisher. Plasmid DNA, pUC18 (1 μg μL^{-1}), was obtained from Bayou Biolabs. Sodium azide (99%) was obtained from Alfa Aesar, D_2O (99.9%) was obtained from Aldrich, and superoxide dismutase (SOD) from bovine erythrocytes was obtained from Sigma. All aqueous solutions were prepared using doubly distilled water. The spectroscopic titrations were carried out at room temperature in the buffer (5 mM Tris-HCl, 0.05 M NaCl, pH 7). The concentrations of the calf-thymus (ct) DNA (Sigma) solutions used in the titrations were determined spectrophotometrically using the extinction coefficient 6600 M^{-1} cm^{-1} at 260 nm. Elemental analyses were performed by Atlantic Microlab. Mass spectral measurements were made at the Mass Spectrometry and Proteomics Facility at The Ohio State University. ^{1}H NMR spectra were recorded on a Bruker 300 MHz NMR spectrophotomer at 298 K.

Synthesis. The syntheses of *cis*-dichlorobis(2,2′-bipyridine)-ruthenium(II) [$Ru(bpy)_2Cl_2$][39] and 1,10-phenanthrolinopyrrole (php)[40] were performed as previously described.

1. 3-Methoxy-4-(hydroxyphenyl)diphenanthropyrromethane [(php)$_2$Van]. In approximately 8 mL of acetic acid was dissolved 0.300 g (1.37 mmol) of php and 0.417 g (2.74 mmol) of 3-methoxy-4-hydroxybenzaldehyde (vanillin, van). The solution was refluxed open to air for 30 min. Upon cooling to room temperature, approximately 30 mL of distilled water was added, followed by ammonium hydroxide, until the solution had precipitated (ca. 10 mL). The gray/blue precipitate was filtered under vacuum, washed 3 × 30 mL with distilled water, and air-dried. Once dry, the precipitate was dissolved in a minimum of ethanol and chromatographed on silica gel using first chloroform followed by incremental additions of methanol. A blue-purple band eluted from the column with a 5:1 chloroform/methanol mixture. The solvent was removed by rotoevaporation and dried in an oven. Yield: 118 mg (% yield = 30%). Anal. Calcd for $C_{36}H_{24}N_6O_2\cdot 0.5CHCl_3$: C, 69.33; H, 3.91; N, 13.29. Found: C, 69.36; H, 4.00; N, 13.32. ESI-MS. Calcd for [M$^{\bullet+}$]: *m*/*z* 573. Found: *m*/*z* 573. ^{1}H NMR (DMSO): δ 3.67 (s, 3H), 6.59 (d, 1H), 6.75 (d, 1H), 6.89 (s, 1H), 7.03 (s, 1H), 7.23−7.31 (m, 2H), 7.52−7.61 (m, 2H), 7.78 (d, 1H), 7.92 (d, 1H), 8.18 (d, 1H), 8.52−8.63 (m, 5H), 8.75 (d, 2H), 9.02 (s, 1H), 11.19 (s, 2H).

2. 4-(Cyanophenyl)diphenanthropyrromethane [(php)$_2$4CNPh]. In approximately 6 mL of acetic acid was dissolved 0.331 g (1.50 mmol) of php and 0.396 g (3.00 mmol) of 4CNPh. The solution was refluxed open to air for 30 min. Upon cooling to room temperature, approximately 30 mL of distilled water was added, followed by ammonium hydroxide until the solution had precipitated (ca. 10 mL). The gray/green precipitate was filtered under vacuum, washed 3 × 30 mL with distilled water, and air-dried. Once dry, the precipitate was dissolved in a minimum of ethanol and chromatographed on silica gel using first chloroform followed by incremental additions of methanol. A purple band eluted from the column with a 10:1 chloroform/methanol mixture. The solvent was removed by rotoevaporation and dried in an oven. Yield: 85.2 mg (% yield = 21%). Anal. Calcd for $C_{36}H_{21}N_7\cdot 0.33CHCl_3\cdot 0.33CH_3OH$: C, 73.24; H, 3.88; N, 16.16. Found: C, 73.43; H, 3.88; N, 15.76. ESI-MS. Calcd for [M$^{\bullet+}$]: *m*/*z* 552. Found: *m*/*z* 552. ^{1}H NMR (DMSO): δ 7.21−7.31 (m, 2H), 7.44−7.47 (d, 2H), 7.54−7.62 (m, 3H), 7.82−7.88 (m, 3H), 7.93−7.95 (d, 1H), 8.12−8.17 (d, 1H), 8.54−8.58 (dd, 2H), 8.61−8.66 (dd, 2H), 8.74−8.79 (m, 3H), 11.3 (s, 2H).

3. [Ru(bpy)$_2$php]$_2$Van(PF$_6$)$_4$. In a 100 mL round-bottomed flask was added 0.069 g (0.12 mmol) of (php)$_2$Van, 0.117 g (0.242 mmol) of $Ru(bpy)_2Cl_2$, and 80 mL of ethanol. The solution was refluxed for 1.5 h followed by reduction of the volume by ca. 50% by rotoevaporation. The concentrated solution was added to approximately 150 mL of a saturated NH_4PF_6 aqueous solution. The precipitate was vacuum-filtered and allowed to air-dry for 1 h. The orange precipitate was taken up in a minimum of acetonitrile (ca. 5 mL) and added dropwise to 100 mL of diethyl ether. The precipitate was again vacuum-filtered and air-dried. Yield: 180 mg (% yield = 75%). Anal. Calcd for $C_{76}H_{56}N_{14}O_2P_4F_{24}Ru_2\cdot 5H_2O$: C, 44.18; H, 2.85; N, 9.77; F, 21.75. Found: C, 44.11; H, 3.21; N, 9.48; F, 22.03.

4. [Ru(bpy)$_2$php]$_2$4CNPh(PF$_6$)$_4$. In a 100 mL round-bottomed flask was added 0.020 g (0.036 mmol) of (php)$_2$4CNPh, 0.038 g (0.077 mmol) of $Ru(bpy)_2Cl_2$, and 25 mL of ethanol. The solution was refluxed for 1.5 h followed by reduction of the volume by ca. 50% by rotoevaporation. The concentrated solution was added to approximately 100 mL of a saturated NH_4PF_6 aqueous solution. The precipitate was vacuum-filtered and allowed to air-dry for 1 h. The orange precipitate was taken up in a minimum of acetonitrile (ca. 5 mL) and added dropwise to 100 mL of diethyl ether. The precipitate

DOI: 10.1021/ic502340p
Inorg. Chem. 2015, 54, 3139−3147

Scheme 1. Synthesis of Diphenathropyrromethanes

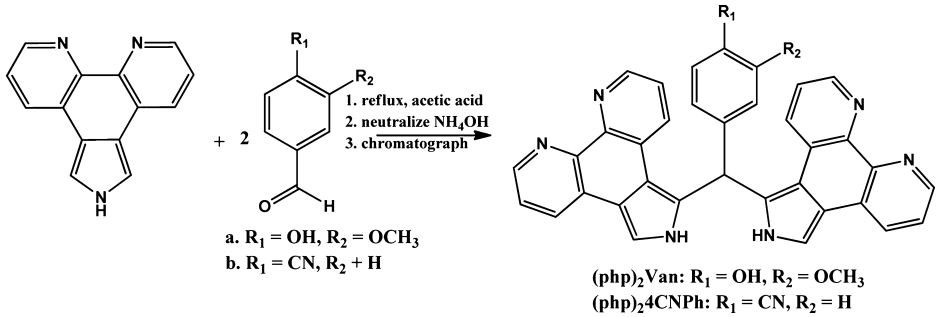

was again vacuum-filtered and air-dried. Yield: 50 mg (% yield = 71%). Anal. Calcd for $C_{76}H_{53}N_{15}P_4F_{24}Ru_2{\cdot}4.5H_2O$: C, 44.71; H, 3.00; N, 10.30. Found: C, 44.33; H, 2.59; N, 9.99.

Electronic Spectroscopy. Electronic absorption spectra were recorded at room temperature using an HP8453 photodiode array spectrophotometer with 2 nm resolution. Because of solubility, the dipyrromethanes were run in ethanol, while the complexes were run in methanol. All spectra were recorded at 298 K.

Emission Spectroscopy. Room temperature luminescence spectra of the dipyrromethanes and ruthenium complexes in a 1 cm quartz spectrophotometer fluorescence cell (Starna) in ethanol and methanol, respectively, were run on a Cary Eclipse fluorescence spectrophotometer.

Electrochemistry. Cyclic voltammograms were recorded under a nitrogen atmosphere using a one-compartment, three-electrode cell (CH Instruments) equipped with a platinum wire auxiliary electrode. The working electrode was a 2.0-mm-diameter glassy carbon disk (CH Instruments), which was first polished using 0.30 μm followed by 0.05 μm alumina polish (Buehler) and then sonicated for 10 s prior to use. Potentials were referenced to a Ag/AgCl electrode (CH Instruments). The supporting electrolyte was 0.1 M Bu_4NPF_6, and the measurements were made in DMF.

Spectroelectrochemistry. Spectroelectrochemical measurements were conducted using a locally constructed H cell, which uses a quartz cuvette as the working compartment. The working and auxiliary compartments were separated by a fine porous glass frit. The working electrode was a high-surface-area platinum mesh, and the auxiliary electrode was a platinum wire. The reference electrode was Ag/AgCl. The measurements were made in 0.1 M $TBAPF_6$/acetonitrile solutions that were millimolar in metal complex in DMF. The electrolysis potential was controlled by a CH Instruments 630A electrochemical analyzer.

DNA Titrations. ct DNA was dissolved in a 5 mM pH 7 tris(hydroxymethyl)aminoethane (Tris) buffer with an ionic strength of 0.05 M in NaCl. Stock solutions of the ruthenium complexes (100 μM) were diluted to 40 μM using the Tris buffer solution. For DNA titrations, 3.0 mL of the diluted ruthenium complexes was placed in 1 cm quartz cuvettes, and aliquots (10 μL) of the ct DNA solution were added. The MLCT transition associated with the Ru($d\pi$) → bpy(π^*) transition was monitored, for both complexes, by electronic absorption spectroscopy.

Plasmid Photocleavage. Buffered solutions of pUC18 and pUC18/ruthenium complexes at a ratio of 5:1 bp/metal complex were placed side by side in quartz cuvettes and irradiated with a 300 W mercury arc lamp (Oriel) equipped with a colored glass filter (Newport FSR-GG420) blocking wavelengths shorter than 550 nm. Samples were taken at 10 min intervals run in 1% agarose gel by applying 150 V for 1 h in approximately 300 mL of a Tris buffer solution. Gels were stained with EthBr and photographed using UV illumination.

RESULTS AND DISCUSSION

From the initial synthesis of dipyrromethanes by Lee and Lindsey[41] in the early 1990s, their importance as building blocks for new and unique porphyrins has been extensively studied. Lash and others have used this technique, along with the method developed by Barton et al.,[42] to make pyrroles with extended π systems, subsequently using these pyrroles to synthesize porphyrins. These porphyrins display significant red shifts in their electronic absorption properties.[43−46] Rillema and co-workers have synthesized a series of ruthenium(II) complexes incorporating php for potential applications in solar energy conversion.[40] Attempts have been made to incorporate this pyrrole into porphyrin molecules but were unsuccessful because of the low nucleophilicity of the pyrrole units resulting from the fused phenanthroline ring.[43] However, the synthesis of tripyranes including one php unit was successful, leading to new porphyrins.

Synthesis: $(php)_2$Van and $(php)_2$4CNPh. Reactions of php with excess aldehyde in acetic acid yielded new dipyrromethanes containing two php units bridged by *meso*-aryl groups (Scheme 1). Column chromatography on silica gel eluted first a faint yellow-green product, followed by a darker reddish-purple band, which required up to 20% methanol in chloroform. The new ligands were obtained in 30% and 21% yield for $(php)_2$Van and $(php)_2$4CNPh, respectively. The identities of the complexes were confirmed by elemental analysis, mass spectroscopy, and ^{1}H NMR. Attempts to increase the yields of the reactions by using excess php, however, were unsuccessful. To our knowledge, dipyrromethanes containing two phenanthroline units linked by an aryl group have not been described. The use of electron-donating (vanillin) and electron-withdrawing (cyano) benzaldehydes does not appear to play a significant role in the reactivity of php toward the aldehydes; however, attempts to use more sterically hindered aldehydes, for example, pentafluorobenzaldehyde, 3,4,5-trimethoxybenzaldehyde, and mesitylbenzaldehyde, did not yield the desired products.

Electronic Absorption and Emission Spectroscopy of the Ligands. Electronic absorption experiments were performed on the ligands in 1 cm quartz fluorescence cuvettes in ethanol. Both ligands show broad absorption bands in the visible region of the spectrum.

The spectrum for $(php)_2$Van appears with a shoulder stretching past 600 nm and an absorption maximum at approximately 514 nm, while the spectrum of $(php)_2$4CNPh has a slightly sharper absorption with a maximum at 519 nm, as in parts A and B of Figure 1 (red lines), respectively. The molar absorptivities of both ligands are relatively low, with $(php)_2$Van having a slightly higher value of 2508 M^{-1} cm^{-1} compared to 1773 M^{-1} cm^{-1} for $(php)_2$4CNPh. Although the molar absorptivities are relatively low, the fact that these ligands absorb in the visible region has not been observed for

DOI: 10.1021/ic502340p
Inorg. Chem. 2015, 54, 3139−3147

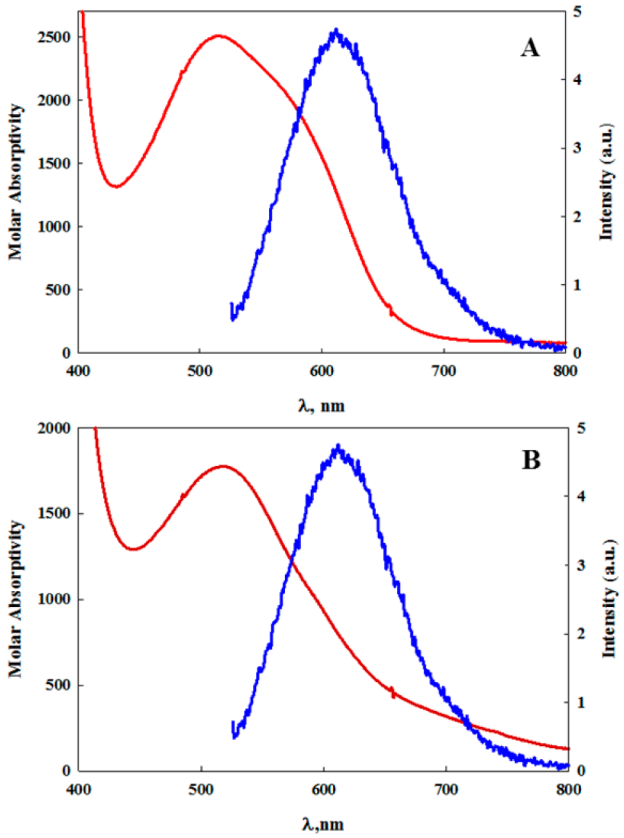

Figure 1. Electronic absorption (red) and emission (blue) spectra for $(php)_2$Van (A) and $(php)_2$4CNPh (B) in ethanol at 298 K.

dipyrromethanes before and indicates that bridging the php units through *meso*-aryl groups plays an important role in the orbital energies of the ligands. When irradiated at their absorption maxima, both ligands give virtually identical weak emission spectra with peaks at 612 nm.

Electrochemistry of the Ligands. Cyclic voltammetry of $(php)_2$Van and $(php)_2$4CNPh was performed in a three-electrode cell with a glassy carbon working electrode, a platinum auxiliary electrode, and a Ag/AgCl reference electrode. The DMF solutions were purged with nitrogen before measurements were taken. Initial scans in the cathodic direction for $(php)_2$Van reveal a well-defined irreversible reduction with E_{pc} = −2.12 V versus Ag/AgCl, followed by a less well-defined irreversible reduction at E_{pc} = −2.56 V versus Ag/AgCl. Upon anodic scanning, an irreversible oxidation wave at E_{pa} = 1.16 V versus Ag/AgCl is observed (solid line in Figure 2). Two well-defined irreversible reduction waves at E_{pc} = −2.24 and −2.57 V versus Ag/AgCl were observed for $(php)_2$4CNPh upon cathodic scanning (dashed line in Figure 2); however, additional smaller irreversible reduction waves were observed between −1.00 and −2.00 V. Further purification of the ligand did not eliminate these reduction waves, which may be the result of minor impurities. In the anodic direction, a broad weak irreversible oxidation wave at approximately 1.00 V versus Ag/AgCl was observed (dashed line in Figure 2). The irreversible oxidation wave observed for $(php)_2$Van is most likely oxidation of the 3-methoxy-4-hydroxyphenyl substituent because this oxidation is not observed for $(php)_2$4CNPh.

Synthesis of Ruthenium Complexes. The bimetallic ruthenium(II) complexes, $[Ru(bpy)_2php]_2Van(PF_6)_4$ and $[Ru(bpy)_2php]_2$4CNPh$(PF_6)_4$, were prepared by the reaction of 1 equiv of $(php)_2$Van or $(php)_2$4CNPh with 2 equiv of $Ru(bpy)_2Cl_2$ in refluxing ethanol.

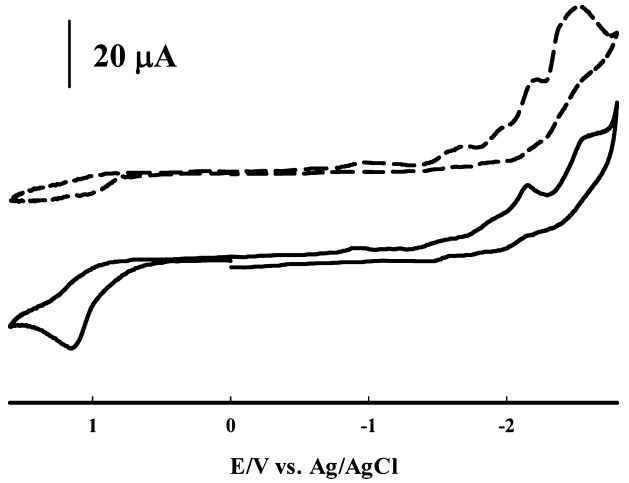

Figure 2. Cyclic voltammetry of $(php)_2$Van (solid line) and $(php)_2$4CNPh (dashed line) in 0.1 M Bu_4NPF_6 in a DMF solution using a glassy carbon working electrode, a platinum wire auxiliary, and a Ag/AgCl reference electrode. Scan rate = 25 mV s^{-1}.

The initial solutions were dark blue-purple but within 20 min of heating turned red-orange, indicating coordination of the ruthenium(II) moiety. The reactions were continued for an additional 1 h to make certain the reaction was complete. Precipitation of the product as the hexafluorophosphate salt was followed by flash precipitation in diethyl ether, resulting in good yields. Elemental analysis agreed with the complexes illustrated in Scheme 2.

Scheme 2. Synthetic Route to $[Ru(bpy)_2php]_2Van(PF_6)_4$ and $[Ru(bpy)_2php]_2$4CNPh$(PF_6)_4$

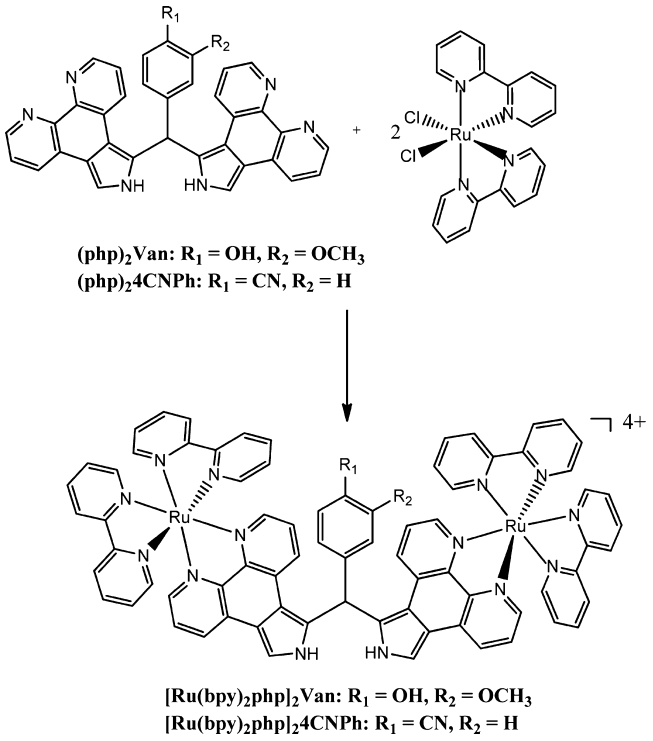

$(php)_2$Van: R_1 = OH, R_2 = OCH_3
$(php)_2$4CNPh: R_1 = CN, R_2 = H

$[Ru(bpy)_2php]_2$Van: R_1 = OH, R_2 = OCH_3
$[Ru(bpy)_2php]_2$4CNPh: R_1 = CN, R_2 = H

DOI: 10.1021/ic502340p
Inorg. Chem. 2015, 54, 3139−3147

Electronic Absorption and Emission Spectroscopy of the Complexes. Electronic absorption spectra were obtained at room temperature in methanol solutions (Figure 3). The

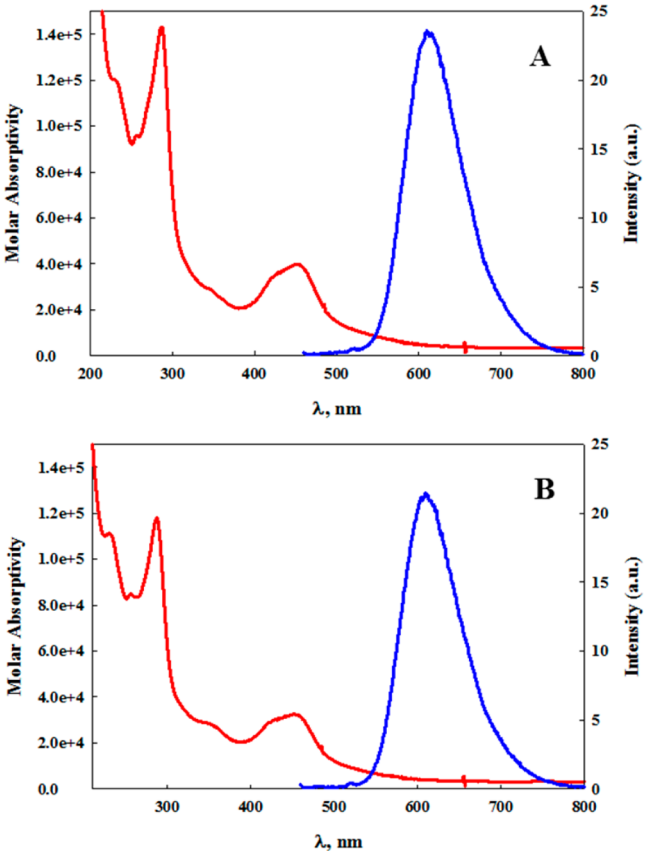

Figure 3. Electronic absorption (red) and emission (blue) spectra for $[Ru(bpy)_2php]_2Van(PF_6)_4$ (A) and $[Ru(bpy)_2php]_24CNPh(PF_6)_4$ (B) in methanol at 298 K. λ_{exc} = 452 nm.

electronic transition, emission, and electrochemical data for both ligands and complexes are listed in Table 1. For comparison, the data for $Ru(bpy)_2php$, as previously described,[40] are also included. The bridged bis-ruthenium complexes display very similar electronic and emission spectra. The ligand-centered (LC; $\pi-\pi^*$) transitions occur at 287 nm, and the MLCT transitions appear at 452 nm. A higher-energy shoulder at ca. 430 nm is associated with overlapping MLCT states.[47] The difference between the complexes lies in their molar absorptivities, with $[Ru(bpy)_2php]_2Van(PF_6)_4$ having considerably higher values at 287 nm ($\Delta\varepsilon$ = 25448 M^{-1} cm^{-1}) and 452 ($\Delta\varepsilon$ = 7255 M^{-1} cm^{-1}) compared to $[Ru(bpy)_2php]_24CNPh(PF_6)_4$. There is no evidence for the electronic transitions of the $(php)_24CNPH$ and $(php)_2Van$ ligands due to their comparatively low molar absorptivities. Emission spectra measured at room temperature upon excitation at 452 nm for both complexes reveal an emission maximum of 610 nm for $[Ru(bpy)_2php]_24CNPh(PF_6)_4$ and a red-shifted emission maximum of 615 nm for $[Ru(bpy)_2php]_2Van(PF_6)_4$.

The emission bands for the bimetallic complexes are red-shifted compared to those of the monometallic $Ru(bpy)_2php^{2+}$ complex, with an emission peak at 606 nm.[40]

Electrochemistry of the Complexes. The electrochemical properties of $[Ru(bpy)_2php]_2Van(PF_6)_4$ and $[Ru(bpy)_2php]_24CNPh(PF_6)_4$ are summarized in Table 1. The cyclic voltammograms of the complexes in deoxygenated DMF solution are virtually identical (Figure 4). Upon cathodic

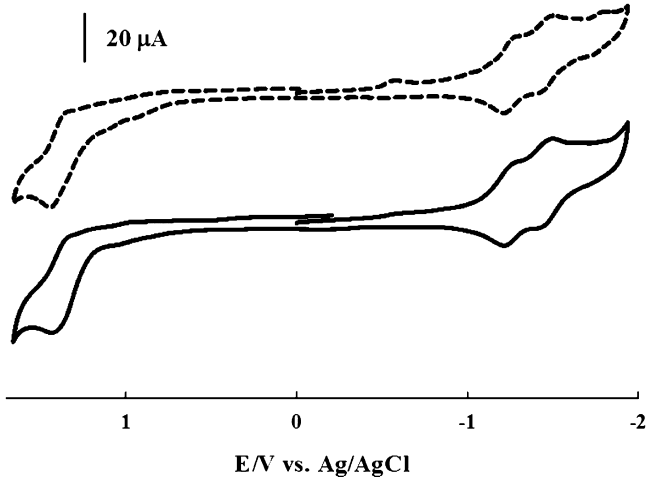

Figure 4. Cyclic voltammograms of $[Ru(bpy)_2php]_2Van(PF_6)_4$ (dotted-line) and $[Ru(bpy)_2php]_24CNPh(PF_6)_4$ (solid line) in 0.1 M Bu_4NPF_6 in a DMF solution using a glassy carbon working electrode, a platinum wire auxiliary, and a Ag/AgCl reference electrode. Scan rate = 100 mV s^{-1}.

scanning, two reversible reduction waves with $E_{1/2}$ values of −1.24 and −1.46 V versus Ag/AgCl are observed for both complexes because of sequential one-electron reductions of the bipyridyl groups. These redox couples are less negative than the corresponding redox couples associated with the monometallic $Ru(bpy)_2php^{2+}$ (Table 1), indicating stabilization of the bipyridyl LUMO orbitals in the case of the bimetallic complexes.

Oxidation of ruthenium(II) in the bimetallic complexes is observed at greater than 1.40 V versus Ag/AgCl for both

Table 1. UV/Vis, Emission, and Redox Properties of the Ligands and Ruthenium(II) Complexes

complex	λ_{max}, nm (ε, M^{-1} cm^{-1})	λ_{max}(em), nm	$E_{1/2}$(oxid), V	$E_{1/2}$(red), V
$(php)_2Van^a$	514 (2508)	612	1.16 (irr)	−2.12 (irr)
$(php)_24CNPh^a$	519 (1773)	612		−2.24 (irr), −2.57 (irr)
$[Ru(bpy)_2php]_2Van(PF_6)_4{}^b$	287 (143191)	615	1.43 (irr)	−1.24
	452 (39754)			−1.46
$[Ru(bpy)_2php]_24CNPh(PF_6)_4{}^b$	287 (117743)	610	1.41 (irr)	−1.24
	452 (32499)			−1.46
$Ru(bpy)_2php^{2+c}$	286 (60740)	606	1.33 (irr)	−1.39
	450 (15230)			−1.64

[a]Spectra run in ethanol; electrochemistry run in DMF. [b]Spectra run in methanol; electrochemistry run in DMF. [c]Taken from ref 40.

DOI: 10.1021/ic502340p
Inorg. Chem. 2015, 54, 3139−3147

complexes (Table 1). The oxidation potential for ruthenium(II) in the bimetallic complexes is approximately 100 mV more positive than that in the monometallic $Ru(bpy)_2php^{2+}$ (Table 1), resulting from greater stabilization of the t_{2g} orbitals by coordination to the phenanthroline-bridged ligands [$(php)_2$4CNPH and $(php)_2$Van].

Spectroelectrochemical experiments were performed on a DMF solution of $[Ru(bpy)_2php]_2Van(PF_6)_4$ to determine if the absence of the LC transition associated with $(php)_2$Van (Figure 1A) is a consequence of coordination to the ruthenium(II) moieties or simply the result of more intense MLCT transitions. Bulk electrolysis of dilute solutions of $[Ru(bpy)_2php]_2Van(PF_6)_4$ in DMF (with Bu_4NPF_6 as the supporting electrolyte) in a quartz cuvette at 1.50 V versus Ag/AgCl [to ensure oxidation of ruthenium(II) to ruthenium(III)] was monitored by spectrophotometry (Figure 5).

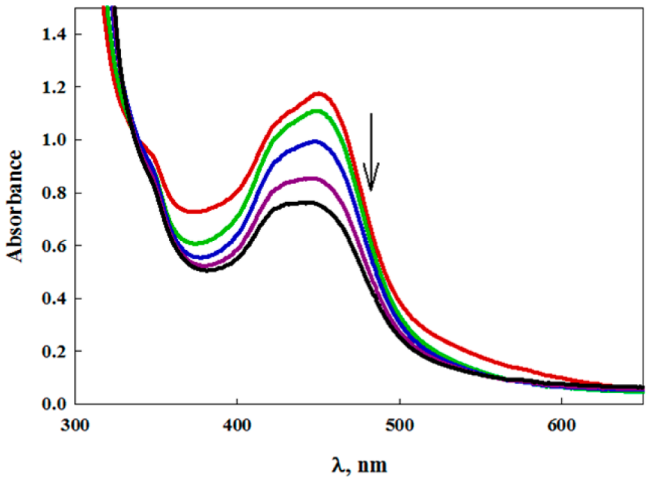

Figure 5. Spectroelectrochemical results for the controlled potential oxidation of $[Ru(bpy)_2php]_2Van(PF_6)_4$ in DMF using a platinum mesh working electrode referenced to a Ag/AgCl electrode.

As ruthenium(II) is oxidized to ruthenium(III), the MLCT observed at 452 nm is reduced and blue-shifted; however, the broad absorption band at 519 nm associated with the $(php)_2$Van LC transition (Figure 1A, red line) did not become evident. Instead, a broad absorption band at ca. 440 nm is observed, representing a blue shift of nearly 80 nm for the LC transition associated with the $(php)_2$Van ligand. This indicates stabilization of the occupied ligand orbitals of $(php)_2$Van upon coordination of the $Ru(bpy)_2Cl_2$ moieties, which explains why oxidation of the $(php)_2$Van ligand is not observed in the cyclic voltammogram of the bimetallic complex (Figure 4, dashed line). When the potential is shifted to 1.00 V versus Ag/AgCl, the original MLCT spectrum is restored, indicating that the ruthenium(III/II) couple initially thought to be irreversible is, in fact, reversible. The isosbestic point at approximately 340 nm is also consistent with the presence of only two species in solution.

The spectroscopic and electrochemical properties of the bimetallic ruthenium complexes are virtually indistinguishable, except for the differences in their molar absorptivities, and display properties similar to those of the monometallic $Ru(bpy)_2php^{2+}$ complex. In addition, unlike more rigidly bridged bimetallic ruthenium complexes,[48] the ruthenium moieties behave independently of each other, and no evidence of dual emission was observed. The absence of the LC transitions associated with the $(php)_2$Van and $(php)_2$4CNPh ligands upon coordination to the ruthenium groups suggests significant overlap of the ligand orbitals with the ruthenium(II) d orbitals.

DNA Titrations. There are a number of ways in which small molecules can interact with DNA, for example, groove binding, which is primarily an electrostatic interaction between a cationic molecule and the negative phosphate backbone of DNA, covalent binding, in which a molecule coordinates to one of the base pairs of DNA (cisplatin covalently binds to DNA), and intercalation, resulting from insertion of the molecule or part of the molecule between the base pairs of DNA. Intercalation typically requires an extended flat aromatic group to accomplish this type of DNA interaction. Because of the intense photophysical properties of ruthenium(II) polypyridyl complexes, a great deal of research has been conducted, beginning with the initial studies by Barton and Turro in the mid-1980s,[49,50] associated with the development of ruthenium(II) complexes as DNA probes and phototherapeutics.[51−57] To this end, we evaluated the interaction of our ruthenium(II) complexes with ct DNA by spectroscopic means.

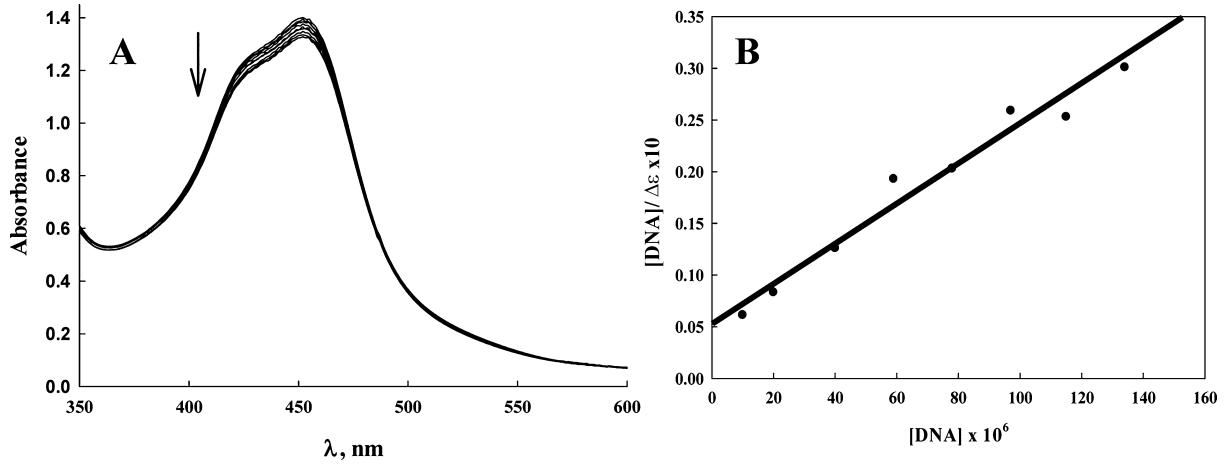

Figure 6. (A) Absorption spectra of a pH 7 buffer solution (ionic strength = 0.05 M) of $[Ru(bpy)_2php]_2Van(PF_6)_4$ in the presence of increasing amounts of ct DNA. [Ru] = 40 μM; [DNA] = 0−140 μM. (B) Plot of [DNA]/$\Delta\varepsilon$ versus [DNA] from eq 1.

DOI: 10.1021/ic502340p
Inorg. Chem. 2015, 54, 3139−3147

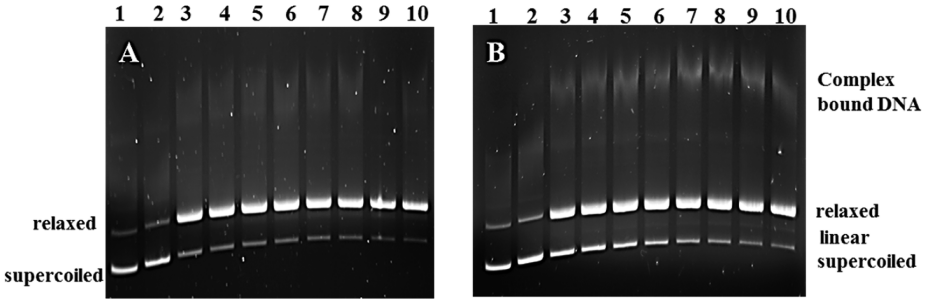

Figure 7. Gel electrophoresis of circular pUC18 in the absence (lane 1) and presence (lanes 2−10) of $[Ru(bpy)_2php]_2$4CNPh (6A) and $[Ru(bpy)_2php]_2$Van (6B) at a 5:1 base pair/complex ratio. Lane 1 represents pUC18 without complex, lane 2 is pUC18 with complex prior to irradiation, and lanes 3−10 represent pUC18 + complex irradiated at 10 min intervals. Samples were irradiated with a 300 W mercury arc lamp equipped with a long pass filter, cutting off wavelengths below 550 nm. Samples were taken at 10 min intervals.

Constant concentrations of $[Ru(bpy)_2php]_2Van(PF_6)_4$ and $[Ru(bpy)_2php]_2$4CNPh$(PF_6)_4$ in aqueous pH 7 solutions (Tris buffer, 0.05 M NaCl) were titrated with ct DNA while being monitored by electronic absorption spectroscopy. An example of the results for one of these experiments is illustrated in Figure 6A. Figure 6B represents a plot of $[DNA]/\Delta\varepsilon$ versus [DNA] according to eq 1,[58] where $\varepsilon_a = A_{obsd}/[Ru]$ and ε_b and ε_f are the molar absorptivities of the fully bound and free form of the ruthenium(II) complexes, respectively.

$$[DNA]/(\varepsilon_a - \varepsilon_f) = [DNA]/(\varepsilon_b - \varepsilon_f) + 1/K_b(\varepsilon_b - \varepsilon_f) \quad (1)$$

As DNA is added to the ruthenium(II) complex solution, both complexes display modest hypochromism of less than 10% for the MLCT transition at 452 nm, which does not shift to lower energy upon the addition of ct DNA. Large hypochromism along with red shifts of greater than 5 nm, in the maximum wavelength, is often associated with intercalation resulting from $\pi-\pi$ stacking of the aromatic groups of the intercalating molecule with the DNA bases; the larger the hypochromism, the greater the binding with DNA. The intrinsic binding constant, determined by dividing the slope of the line by the intercept (Figure 6B), gives a K_b value of $(4.64 \pm 0.97) \times 10^4\ M^{-1}$ for $[Ru(bpy)_2php]_2Van(PF_6)_4$. This is of the magnitude of other ruthenium(II) complexes with extended aromatic systems that have been associated with intercalative processes;[30,50,52,52,57] however, electrostatic binding cannot be ruled out because this molecule carries a 4+ overall charge. Surprisingly, the intrinsic binding constant for $[Ru(bpy)_2php]_2$4CNPh$(PF_6)_4$ was an order of magnitude lower than that for $[Ru(bpy)_2php]_2Van(PF_6)_4$, with a value of $(4.62 \pm 1.02) \times 10^3\ M^{-1}$. An intrinsic binding constant on the order of $10^3\ M^{-1}$ has been reported for $Ru(phen)_3^{2+}$ and was attributed to strong electrostatic interactions.[50]

Both of the complexes in this study are highly charged and therefore most likely involve a strong electrostatic attraction to DNA with an additional weak intercalative process for $[Ru(bpy)_2php]_2Van(PF_6)_4$. Structurally, however, the complexes differ only in the substituents on the phenyl groups of the tetrahedral bridging carbon. Spectroscopic and electrochemical studies suggest that these substituents play little to no role in the observable orbital energies, with the ruthenium(II) d orbitals associated with the highest occupied molecular orbital and the bipyridyl groups associated with the lowest unoccupied molecular orbital. The DNA binding differences may result from the $[Ru(bpy)_2php]_2Van(PF_6)_4$ complex having a distal hydroxyl group capable of hydrogen bonding with the phosphate backbone; however, more detailed studies are needed to justify this assumption.

Photocleavage of pUC18. Aqueous solutions of $[Ru(bpy)_2php]_2Van(PF_6)_4$ and $[Ru(bpy)_2php]_2$4CNPh$(PF_6)_4$ were combined with pUC18 at a ratio of 5:1 base pairs/complex. The solutions were irradiated with a 300 W mercury arc lamp equipped with a long-band-pass 550 nm filter, preventing light of shorter wavelengths from penetrating the solutions. Samples were taken at 10 min intervals and run on gel electrophoresis to determine the extent of photoinduced DNA damage (Figure 6). Supercoiled DNA with its high electron density travels the farthest through the gel; if single-strand breaks in the DNA occur, the tightly coiled DNA relaxes, giving a larger surface area and slower movement through the gel. If double-strand breaks occur, the circular plasmid becomes linearized and travels through the gel at a speed intermediate to the supercoiled and relaxed forms.

Lane 1 (Figure 7A,B) represents pUC18 without complex in the dark. Experiments on pUC18, in the absence of complex, irradiated for 1 h under the same conditions as those above did not show any photonicking. Lane 2 (Figure 7A) represents pUC18 with $[Ru(bpy)_2php]_2$4CNPh$(PF_6)_4$ at a 5:1 base pair/complex ratio without irradiation. A slight retardation in the migration is observed compared to the control lane 1, indicating some binding of the complex to the DNA. Lanes 3−10 (Figure 7A) represent the mixture of pUC18 and $[Ru(bpy)_2php]_2$4CNPh$(PF_6)_4$ at a 5:1 base pair/complex ratio, irradiated with light of wavelengths higher than 550 nm, with sample aliquots taken at 10 min intervals. After only 10 min of irradiation, the majority of pUC18 has been photonicked, and after 80 min, complete nicking is observed. In the case of the $[Ru(bpy)_2php]_2Van(PF_6)_4$ mixture with pUC18 at a 5:1 base pair/complex ratio (Figure 7B), photonicking of the DNA takes place in the first 10 min of irradiation, but after 80 min of irradiation, there is still some of the circular plasmid visible in the gel. However, after 50 min of irradiation, there is some evidence of the linear form of DNA resulting from double-strand breaks. It is also interesting to note that, in Figure 7B, after 10 min of irradiation, a band begins to appear near the gel wells. This slow-moving band is indicative of highly bound DNA with the complex and interestingly does not appear in lane 2 (Figure 7B) when the DNA is in the presence of the complex without irradiation. As the irradiation continues, this band seems to become darker, indicating that more DNA is being bound. On the basis of this experiment, it seems apparent that this highly bound form of DNA only occurs upon irradiation of the samples, suggesting a mechanism by which

DOI: 10.1021/ic502340p
Inorg. Chem. 2015, 54, 3139−3147

the complex is accessing the ^{3}MC state, leading to photosubstitution.[59−62]

Photoinduced single- and double-strand DNA nicking typically occurs by one of two mechanisms. In PDT, the most common mechanism is the transfer of energy from the excited photosensitizer to triplet oxygen, creating reactive singlet oxygen. Another mechanism is direct electron transfer from the excited photosensitizer to either oxygen or other biological molecules, creating reactive oxygen species (ROS), for example, superoxide or hydroxyl radicals. To test the photoinduced mechanism of $[Ru(bpy)_2php]_2Van^{4+}$ and $[Ru(bpy)_2php]_24CNPh^{4+}$, the photolysis reactions were repeated using a 300 W mercury arc lamp equipped with a 550 nm filter. Aqueous solutions of pUC18 and the complexes were irradiated for 15 min. Samples contained, in addition to the complexes and pUC18, inhibitors capable of trapping ROS or quenching singlet oxygen. Gel electrophoresis was used to determine the effects of the inhibitors on DNA nicking, the results of which are illustrated in Figure 8.

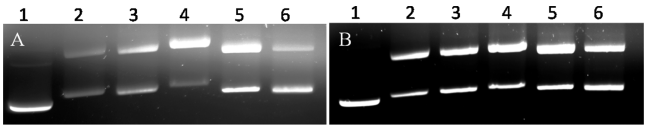

Figure 8. Photoinduced cleavage of pUC18 in the presence of (A) $[Ru(bpy)_2php]_24CNPh^{4+}$ and (B) $[Ru(bpy)_2php]_2Van^{4+}$ at a 5:1 base pair/complex ratio and different inhibitors after irradiation with a 300 W mercury arc lamp equipped with a 550 nm filter. Lane 1 (A and B): pUC18 in the absence of complex, inhibitor, and irradiation. Lane 2 (A and B): pUC18 and complex, no inhibitor, irradiated for 15 min. Lane 3: in the presence of DMSO (200 mM). Lane 4: in the presence of D_2O (99.9%). Lane 5: in the presence of sodium azide (10 mM). Lane 6: in the presence of SOD (ca. 3000 U mL^{-1}).

In the presence of DMSO, a strong hydroxyl radical scavenger, there appears to be little difference, for either complex, in the amount of nicked pUC18 formed (Figure 8A,B, lane 3) compared to the observed photonicking in the absence of DMSO (Figure 8A,B, lane 2). In lane 4, the presence of D_2O (which prolongs the lifetime of singlet oxygen) shows significant enhancement in the formation of the photonicked DNA in both complexes, but a greater enhancement is observed for $[Ru(bpy)_2php]_24CNPh^{4+}$ (Figure 8A). This indicates that singlet oxygen is at least partially responsible for the photonicking of DNA. When the reactions are repeated in the presence of sodium azide (a singlet oxygen quencher; Figure 8A,B, lane 5), both complexes show an increase of photonicking compared to photonicking in the absence of inhibitor (Figure 8A,B, lane 2). This is counterintuitive based on the D_2O results and suggests a more complex mechanism of photonicking. In the presence of SOD, a superoxide radical scavenger, $[Ru(bpy)_2php]_24CNPh^{4+}$ shows a marked decrease in the formation of the nicked form of pUC18 (Figure 8A, lane 6), while a decrease in photonicking, but to a lesser extent, is also observed for $[Ru(bpy)_2php]_2Van^{4+}$ (Figure 8B, lane 6). What seems clear from these results is that in the excited state both ruthenium complexes generate singlet oxygen and superoxide radicals. This dual mechanism has been observed for monometallic tris(bipyrazyl)ruthenium(II).[63] The increase in photonicking in the presence of the singlet oxygen scavenger sodium azide suggests that superoxide plays a more significant role in the photonicking. If the presence of singlet oxygen somehow interferes with the superoxide radical, then upon removal of the singlet oxygen, it would be expected that photonicking would be enhanced. The observation of enhanced photonicking in the presence of D_2O indicates that the singlet oxygen reverts to the ground state before it reaches the DNA unless its lifetime is enhanced, as is the case in D_2O. This is consistent with the observation that there is greater enhancement with the weaker binding molecule $[Ru(bpy)_2php]_24CNPh^{4+}$ (Figure 8A, lane 4).

CONCLUSIONS

This report illustrates the straightforward synthesis of two new bis(php) bridging ligands and their ability to coordinate to ruthenium(II) bis(bipyridyl) groups. The electronic spectroscopy and cyclic voltammetry of the ruthenium(II) complexes are similar to those of monometallic complexes containing the php ligand, indicating that the saturated bridging groups allow the ruthenium moieties to behave independently. The luminescent and emissive properties of the ligands are believed to shift to higher energy upon coordination of the ruthenium groups. These new ligand systems are to our knowledge unprecedented in terms of their photophysical properties. Both complexes show relatively weak interactions with ct DNA, suggesting electrostatic interactions resulting from their high cationic charge and their bulky geometry. Aqueous solutions of the complexes in the presence of pUC18 show the ability to photoreact when irradiated with wavelengths past the MLCT transitions observed by spectroscopic experiments, indicating the ability to access the MLCT states even at lower energy. With continued irradiation, $[Ru(bpy)_2php]_2Van(PF_6)_4$ shows the ability to photocleave pUC18, and in addition, there is evidence that this complex undergoes a photoinduced binding mode toward pUC18. The mechanism of photoreaction with pUC18 appears to result from both energy transfer (singlet oxygen formation) and electron transfer (superoxide radical formation). The synthetic route presented will be used to obtain a variety of bridging ligands capable of coordinating other transition and lanthanide metals for potential application as solar energy sources, light-induced therapeutics, and biosensors/bioprobes.

AUTHOR INFORMATION

Corresponding Author

*Tel.: 1-937-229-3145. Fax: 1-937-229-2635. E-mail: sswavey1@udayton.edu.

Notes

The authors declare no competing financial interest.

REFERENCES

(1) Gambino, D.; Otero, L. *Inorg. Chim. Acta* **2012**, *393*, 103−114.
(2) Iniguez, E.; Sanchez, A.; Vasques, M. A.; Martinex, A.; Olivas, J.; Sattler, A.; Sanchez-Delgado, R. A.; Rosa, A. *J. Biol. Inorg. Chem.* **2013**, *18*, 779−790.
(3) Martinez, A.; Carreon, T.; Iniguez, E.; Anzellotti, A.; Sanchez, A.; Tyan, M.; Sattler, A.; Herrera, L.; Maldonado, R. A.; Sanchez-Delgado, R. A. *J. Med. Chem.* **2012**, *55*, 3867−3877.
(4) Pizarro, A. M.; Sadler, P. J. *Biochemie* **2009**, 1198−1211.
(5) Wang, F.; Bella, J.; Parkinson, J. A.; Sadler, P. J. *J. Biol. Inorg. Chem.* **2005**, *10*, 147−155.
(6) Chatterjee, S.; Kunda, S.; Bhattacharyya, A.; Hartinger, C. G.; Dyson, P. J. *J. Biol. Inorg. Chem.* **2008**, *13*, 1149−1155.
(7) Bergamo, A.; Sava, G. *Dalton Trans.* **2011**, *40*, 7817−7823.
(8) Ang, W. H.; Daldini, E.; Scolaro, C.; Scopelliti, R.; Juillerat-Jeannerat, L.; Dyson, P. J. *Inorg. Chem.* **2006**, *45*, 9006−9013.

DOI: 10.1021/ic502340p
Inorg. Chem. 2015, 54, 3139−3147

(9) Pastorekova, S.; Zatovicova, M.; Pastorek, J. *Curr. Pharm. Des.* **2008**, *14*, 685−698.
(10) Nagy, E. M.; Pettenuzzo, A.; Boscutti, G.; Marchio, L.; Dalla Via, L.; Fregona, D. *Chem.—Eur. J.* **2012**, *18*, 14464−14472.
(11) Hartinger, C. G.; Jakupec, M. A.; Zorbas-Seigfried, S.; Groessl, M.; Egger, A.; Berger, W.; Zorbas, H.; Dyson, P. J.; Keppler, B. K. *Chem. Biodiversity* **2008**, *5*, 2140−2154.
(12) Domotor, O.; Hartinger, C. G.; Bytzek, A. K.; Keppler, B. K.; Enyedy, E. A. *J. Biol. Inorg. Chem.* **2013**, *18*, 9−17.
(13) Alessio, E.; Mestroni, G.; Bergamo, A.; Sava, G. *Curr. Trends Med. Chem.* **2004**, *4*, 1525−2535.
(14) Nazarov, A. A.; Hartinger, C. G.; Dyson, P. J. *J. Organomet. Chem.* **2014**, *751*, 251−260.
(15) Kljun, J.; Bratsos, I.; Alessio, E.; Psomas, G.; Repnik, U.; Butinar, M.; Turk, B.; Turel, I. *Inorg. Chem.* **2013**, *52*, 9039−9052.
(16) De Paulo Silveira-Lacerda, E.; et al. *Biol. Trace Elem. Res.* **2010**, *133*, 270−283.
(17) Alessio, E.; Mestroni, G.; Bergamo, A.; Sava, G. *Curr. Trends Med. Chem.* **2004**, *4*, 1525−2535.
(18) Reedijk, J. *Platinum Met. Rev.* **2008**, *52*, 2−11.
(19) Juris, A.; Balzani, V.; Barigelletti, F.; Campagna, S.; Belser, P.; Von Zelewsky, A. *Coord. Chem. Rev.* **1988**, *84*, 85−277.
(20) Rillema, D. P.; Blanton, C. B.; Shaver, R. J.; Jackman, D. C.; Boldaji, M.; Bundy, S.; Worl, L. A.; Meyer, T. J. *Inorg. Chem.* **1992**, *31*, 1600−1606.
(21) Tfouni, E. *Coord. Chem. Rev.* **2000**, *196*, 281−305.
(22) Moucheron, C.; Kirsch-De Mesmaeker, A.; Kelly, J. M. *J. Photochem. Photobiol., B* **1997**, *40*, 91−106.
(23) Feeney, M. M.; Kelly, J. M.; Tossi, A. B.; Kirsch-De Mesmaeker, A.; Lecomte, J. P. *J. Photochem. Photobiol., B* **1994**, *23*, 69−78.
(24) Lecomte, J. P.; Kirsch-De Mesmaeker, A.; Kelly, J. M. *Bull. Soc. Chim. Belg.* **1994**, *103*, 193−200.
(25) Rillema, D. P.; Allen, G.; Meyer, T. J.; Conrad, D. *Inorg. Chem.* **1983**, *22*, 1617−1622.
(26) Kirsch-De Mesmaeker, A.; Nasieski-Hinkens, R.; Maetens, D.; Pauwels, D.; Nasielski, J. *Inorg. Chem.* **1984**, *23*, 377−379.
(27) Masschelein, A.; Kirsch-De Mesmaeker, A.; verhoeven, C.; Nasielski-Hinkens, R. *Inorg. Chim. Acta* **1987**, *129*, L13−L16.
(28) Kirsch-De Mesmaeker, A.; Jacquet, L.; Masschelein, A.; Vanhecke, F.; Heremans, K. *Inorg. Chem.* **1989**, *28*, 2465−2470.
(29) Jacquet, L.; Kirsch-De Mesmaeker, A. *J. Chem. Soc., Faraday Trans.* **1992**, *88*, 2471−2480.
(30) Pyle, A. M.; Rehmann, J. P.; Meshoyrer, R.; Kumar, C. V.; Turro, N. J.; Barton, J. K. *J. Am. Chem. Soc.* **1989**, *111*, 3051−3058.
(31) Grover, N.; Welch, T. W.; Fariley, T. A.; Cory, M.; Thorp, H. H. *Inorg. Chem.* **1994**, *33*, 3544−3548.
(32) Vanderlinden, W.; Blunt, M.; David, C. C.; Moucheron, C.; Kirsch-De Mesmaeker, A.; De Feyter, S. *J. Am. Chem. Soc.* **2012**, *134*, 10214−10221.
(33) Servaty, K.; Moucheron, C.; Kirsch-De Mesmaeker, A. *Dalton Trans.* **2011**, *40*, 11704−11711.
(34) D'Alessandro, D. M.; Keene, F. R. *Chem.—Eur. J.* **2005**, *11*, 3679−3688.
(35) Zhou, R.; Sedai, B.; Manbeck, G. F.; Brewer, K. J. *Inorg. Chem.* **2013**, *52*, 13314−13324.
(36) Holder, A. A.; Swavey, S.; Brewer, K. J. *Inorg. Chem.* **2004**, *43*, 303−308.
(37) Kwon, B.-H.; Choi, B.-H.; Lee, H. M.; Jang, Y. J.; Lee, J. C.; Kim, S. K. *Bull. Korean Chem. Soc.* **2010**, *31*, 1615−1620.
(38) McDonnell, U.; Hicks, M. R.; Hannon, M. J.; Rodger, A. *J. Inorg. Biochem.* **2008**, *102*, 2052−2059.
(39) Sullivan, B. P.; Salmon, D. J.; Meyer, T. J. *Inorg. Chem.* **1978**, *17*, 3334−3341.
(40) Villegas, J. M.; Stoyanov, S. R.; Rillema, D. P. *Inorg. Chem.* **2002**, *41*, 6688−6694.
(41) Lee, C. H.; Lindsey, J. S. *Tetrahedron* **1994**, *50*, 11427−11440.
(42) Barton, D. H. R.; Kervagoret, J.; Zard, S. Z. *Tetrahedron* **1990**, *46*, 7587−7598.
(43) Lash, T. D.; Lin, Y.; Novak, B. H.; Parikn, M. D. *Tetrahedron* **2005**, *61*, 11601−11614.
(44) Xu, H. J.; Mack, J.; Descalzo, A. B.; Shen, Z.; Kobayashi, N.; You, X. Z.; Rurack, K. *Chem.—Eur. J.* **2011**, *17*, 8965−8983.
(45) Xu, H. J.; Shen, Z.; Okujima, T.; Ono, N.; You, X. Z. *Tetrahedron Lett.* **2006**, *47*, 931−934.
(46) Spence, J. D.; Lash, T. D. *J. Org. Chem.* **2000**, *65*, 1530−1539.
(47) Glazer, E. C.; Magde, D.; Tor, Y. *J. Am. Chem. Soc.* **2007**, *129*, 8544−8551.
(48) Glazer, E. C.; Magde, D.; Tor, Y. *J. Am. Chem. Soc.* **2005**, *127*, 4190−4192.
(49) Kumar, C. V.; Barton, J. K.; Turro, N. J. *J. Am. Chem. Soc.* **1985**, *107*, 5518−5523.
(50) Barton, J. K.; Goldberg, J. M.; Kumar, C. V.; Turro, N. J. *J. Am. Chem. Soc.* **1986**, *108*, 2081−2088.
(51) Friedman, A. E.; Chambron, J. C.; Sauvage, J. P.; Turro, N. J.; Barton, J. K. *J. Am. Chem. Soc.* **1990**, *112*, 4960−4962.
(52) Gao, F.; Chao, H.; Zhou, F.; Yuan, Y. X.; Peng, B.; Ji, L. N. *J. Inorg. Biochem.* **2006**, *100*, 1487−1494.
(53) Zhen, Q. X.; Ye, B. H.; Zhang, Q. L.; Liu, J. G.; Li, H.; Ji, L. N.; Want, L. *J. Inorg. Biochem.* **1999**, *76*, 47−53.
(54) Malina, J.; Hannon, M. J.; Brabec, V. *Nucleic Acids Res.* **2008**, *36*, 3630−3638.
(55) Malina, J.; Hannon, M. J.; Brabec, V. *Chem.—Eur. J.* **2008**, *14*, 10408−10414.
(56) Triantafillidi, K.; Karidi, K.; Malina, J.; Garoufis, A. *Dalton Trans.* **2009**, 6403−6415.
(57) Zhen, Q. X.; Zhang, Q. L.; Liu, J. G.; Ye, B. H.; Ji, L. N.; Wang, L. *J. Inorg. Biochem.* **2000**, *78*, 293−298.
(58) Assefa, Z.; Vantieghem, A.; Deelereq, Q.; Vandenabeele, P.; Vandenheede, J. R.; Merlevede, W.; deWitte, P.; Agostinis, P. *J. Biol. Chem.* **1999**, *274*, 8788.
(59) Sears, R. B.; Joyce, L. E.; Ojaimi, M.; Gallucci, J. C.; Thummel, R. P.; Turro, C. *J. Inorg. Biochem.* **2013**, *121*, 77−87.
(60) Hurley, D. J.; Tor, Y. *J. Am. Chem. Soc.* **2002**, *124*, 3749−3762.
(61) Singh, T. N.; Turro, C. *Inorg. Chem.* **2004**, *43*, 7260−7262.
(62) Chen, H.; Parkinson, J. A.; Parsons, S.; Coxall, R. A.; Gould, R. O.; Sadler, P. J. *J. Am. Chem. Soc.* **2002**, *124*, 3064−3082.
(63) Gicquel, E.; Paillous, N.; Vicendo, P. *Photochem. Photobiol.* **2000**, *72*, 583−589.

DOI: 10.1021/ic502340p
Inorg. Chem. 2015, 54, 3139−3147